


Proceedings Article

An Arbitrary Waveform MPI Scanner

Beril Alyuz ^{1,2,*} · Musa Tunc Arslan ^{1,2} · Mustafa Utkur ^{1,2} · Emine Ulku Saritas ^{1,2,3}

¹Department of Electrical and Electronics Engineering, Bilkent University, Ankara, Turkey

²National Magnetic Resonance Research Center (UMRAM), Bilkent University, Ankara, Turkey

³Neuroscience Program, Sabuncu Brain Research Center, Bilkent University, Ankara, Turkey

*Corresponding author, email: beril@ee.bilkent.edu.tr

© 2022 Alyuz *et al.*; licensee Infinite Science Publishing GmbH

This is an Open Access article distributed under the terms of the Creative Commons Attribution License (<http://creativecommons.org/licenses/by/4.0>), which permits unrestricted use, distribution, and reproduction in any medium, provided the original work is properly cited.

Abstract

In magnetic particle imaging (MPI) systems, impedance matching or tuning circuitry has to be employed at a particular operating frequency to handle the reactive power. In this work, we propose a drive coil design with a Rutherford cable winding comprised of 12 Litz wires twisted together to enable arbitrary waveform (AW) characteristics in an MPI scanner. The AW drive coil achieves a 144-fold reduction in inductance and 12-fold reduction in voltage to generate a given drive field amplitude, compared to a standard drive coil with regular Litz wire windings. With imaging experiments, we show that the proposed design can enable imaging in a wide bandwidth, providing flexibility for different functional imaging applications of MPI.

I. Introduction

Magnetic particle imaging (MPI) scanners utilize drive fields (DF) to excite magnetic nanoparticles (MNP) and image their spatial distribution. Typical MPI scanners handle the reactive power on the drive coil via impedance matching circuitry tuned to a single resonant frequency. The necessity for such circuitry limits the flexibility of the imaging system, restricting it to a particular operating frequency. However, the optimal frequency may be different for functional imaging applications of MPI [1].

Reducing the reactive power on the power amplifier is necessary to achieve DF amplitudes large enough to excite the MNPs. One method to reduce the reactive power for a wide bandwidth is miniaturizing the drive coil to reduce its inductance [2]. Reduced inductance eliminates the need for impedance matching, enabling arbitrary waveform (AW) characteristics. Previous studies achieved AW characteristics for magnetic particle spectrometer (MPS) and relaxometer setups [2–4]. Additionally, a small-scale field free line (FFL) MPI scanner was constructed by adding magnets to an AW relaxometer to enable pulsed excitation in MPI [5]. While employing

small-scale coils is feasible for such setups, typical MPI scanners have considerably larger dimensions.

In this work, we propose an AW drive coil design to achieve AW characteristics in an MPI scanner. The proposed design utilizes Rutherford cable windings to achieve a 144-fold reduction in inductance compared to a standard drive coil. Low inductive reactance enables functionality in a wide range of frequencies without a need for impedance matching or tuning circuitry. Proof-of-concept results are demonstrated via imaging experiments on an FFL scanner with two distinct sinusoidal DF waveforms at 2.5kHz and 5kHz.

II. Material and Methods

II.I. Arbitrary Waveform Drive Coil

To obviate the need for impedance matching at a specific DF frequency, we propose an AW drive coil that utilizes Rutherford cable windings. This design can considerably reduce the inductance of the drive coil and hence the reactive power that the power amplifier needs to supply.

Table 1: Comparison of coil specifications for a standard drive coil and an AW drive coil

	Simulated Standard Drive Coil	Simulated AW Drive Coil	Measured AW Drive Coil
Inner Radius	22 mm	22 mm	22 mm
Coil Length	93.6 mm	93.6 mm	93.6 mm
# of Layers	10	5	5
Inductance	8.48 mH	56.95 μ H	46.97 μ H
DC Resistance	6.7 Ω	40.7 m Ω	37.5 m Ω
Coil Sensitivity at 5 kHz	6.2 mT/A	0.51 mT/A	0.36 mT/A
Voltage at 5 kHz, 7 mT	302.5 V	25.6 V	28.71 V

To form Rutherford cable windings, N_R Litz wires are twisted together to form a single cable with a rectangular cross-section. Since the number of winding is reduced N_R -fold using this cable, the inductance is reduced N_R^2 -fold, and the voltage on the coil is reduced N_R -fold [6].

Table 1 lists the specifications of the AW drive coil, comparing it with a simulated standard drive coil of identical diameter and length but with regular Litz wire windings. In our design, we chose N_R as 12. The Rutherford cable was prepared using 125/40 AWG Litz wires, twisted together to form a 6×2 rectangular cross-section. The AW drive coil had 5 layers with 13 Rutherford cable windings per layer. The separation between the drive coil and the copper shield played a critical role in determining the number of layers, since the copper shield reduces the drive coil sensitivity as the separation gets smaller. For our in-house MPI scanner, 5 layers provided a favorable trade-off between high coil sensitivity and reduced coil inductance, achieving functionality in a wide range of frequencies within the hardware limits.

II.II. Simulations

The designed AW drive coil was simulated in COMSOL Multiphysics @Version 5.5. There is no publicly available method to simulate Rutherford cable windings in COMSOL. Here, we utilized a 2D axisymmetric model, and simulated each 6×2 cross-section of the Rutherford cable as a single solid wire. The copper shield of our in-house MPI scanner was also incorporated into these simulations to account for the shielding effects. The goal of these simulations was to predict the coil performance in terms of coil sensitivity, inductance, and resistive heating. To this end, a Frequency-Transient study was utilized to compute the temperature changes over time and the electromagnetic field distribution as a function of operating frequency. Electromagnetic field distribution and temperature changes were simulated using Magnetic Fields and Heat Transfer in Solids interfaces, respectively. The coil sensitivity was simulated at 2.5 kHz and 5 kHz. The resistive heating was simulated for a DF duration of 90 s and amplitude of 7 mT, at 2.5 kHz and 5 kHz. The duration of 90 s was chosen as it corresponded to the scan

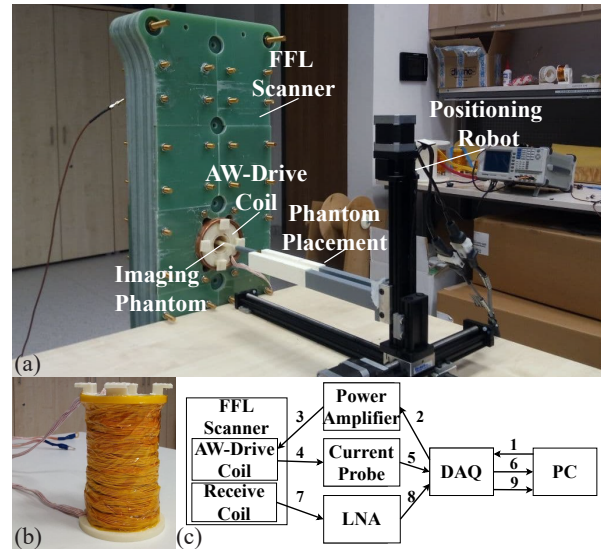


Figure 1: (a) In-house FFL MPI scanner and (b) AW drive coil. (c) Imaging procedure. Arrows 1-6: Adjustment of the input voltage according to a baseline acquisition and desired DF amplitude. The PC sends a signal using DAQ to power amplifier, which amplifies the signal and feeds it to AW drive coil. The current through the AW drive coil is measured with a current probe. Arrows 7-9: MPI signal acquisition during imaging.

time utilized in the imaging experiments.

II.III. Imaging Experiments

The imaging experiments were performed on our in-house FFL MPI scanner, shown in Fig. 1a. This scanner performed projection format imaging and had selection field gradients of $(-4.4, 0, 4.4)$ T/m, and a free imaging bore size of 3.6 cm [7]. The implemented AW drive coil is shown in Fig. 1b, with the measured specification given in Table 1. The receive coil was a doubly tunable gradiometer coil that had fine- and coarse-tuning adjustments [8]. This feature enabled high tuning sensitivity at different operating frequencies. The imaging procedure is explained in Fig. 1c. The DF waveform was sent to a power amplifier (AE Techron 7224) through a data acquisition card (DAQ) (NI USB-6383). The power amplifier was directly connected to the AW drive coil without the need for impedance matching. The current through the AW drive coil was calibrated using a current probe (LFR 06/6/300, PEM) before each experiment. The received signal was amplified with a low-noise voltage pre-amplifier (LNA) (SRS SR560) and sent to a PC via the DAQ. The entire setup was controlled using MATLAB.

The imaging phantom contained two samples: 30 μ l 10-fold diluted Perimag MNPs with 1.7 mg Fe/mL concentration and 30 μ l undiluted Vivotrax MNPs with 5.5 mg Fe/mL concentration. A 2D line-by-line trajectory was utilized to cover a FOV of size 1.7×5.4 cm² in the x-z plane, with a total scan time of 76 s. This FOV was

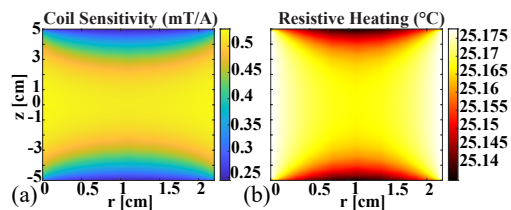


Figure 2: COMSOL simulation results for the AW drive coil. (a) The coil sensitivity at 5 kHz, and (b) the resistive heating after continuously applying the DF for 90 s at 5 kHz and 7 mT.

covered in 18 lines along the z -direction, distanced 1 mm apart from each other. Imaging was performed at two different sinusoidal DF waveforms at 2.5 kHz and 5 kHz, with a fixed amplitude of 7 mT. The MPI images were reconstructed using Partial FOV Center Imaging (PCI), a robust x -space based reconstruction algorithm [9].

III. Results and Discussion

The results of coil sensitivity and resistive heating simulations are given in Fig. 2 for 5 kHz only. The simulated resistive heating remained negligible after continuously applying the DF for 90 s, indicating that no external cooling is required. The performances remained almost identical at 2.5 kHz.

In Table 1, the simulated AW drive coil achieves approximately 12-fold reduction in the required voltage and 144-fold reduction in the coil inductance, when compared to the standard drive coil. The Rutherford cable winding reduces both the DC resistance and the inductance, scaling down the required voltages. The reduced coil sensitivity of the AW drive coil indicates higher current requirements, which creates a hardware limitation for the DF amplitude. The specifications for the simulated and measured AW drive coils match closely. The slight deviations may stem from the simulation approach for Rutherford cable winding, as well as the non-idealities in the cable and coil implementation.

The imaging experiment results are shown in Fig. 3, along with the imaging phantom. The signal level at 2.5 kHz was approximately half of that at 5 kHz, which caused slightly increased background artifacts at 2.5 kHz. These results demonstrate that the proposed AW MPI scanner can image successfully at different frequencies without any impedance matching.

IV. Conclusion

In this work, we proposed an AW MPI scanner and demonstrated successful imaging results at two different DF frequencies. The proposed AW drive coil utilizes Rutherford cable windings to achieve a small inductance needed for AW characteristics. By eliminating the need

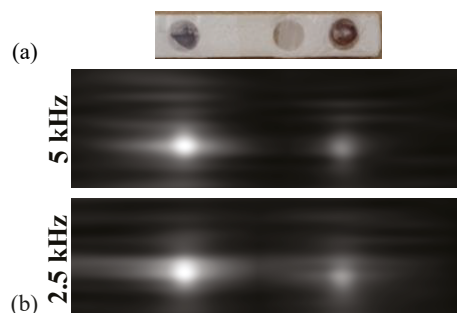


Figure 3: Imaging experiment results for AW MPI scanner. (a) The imaging phantom containing two samples placed at 2.3 cm separation. (b) Projection format MPI images at 5 kHz and 2.5 kHz. FOV was $1.7 \times 5.4 \text{ cm}^2$ in the x - z plane.

for matching circuitry, this design enables imaging at a wide range of frequencies, providing flexible operation for functional imaging applications of MPI.

Acknowledgments

The authors thank Ali Alper Özasan for his help with Rutherford cable preparation and Elif Aygün for her help with 3D printing. This work was supported by the Scientific and Technological Research Council of Turkey (Grant No: TUBITAK 120E208).

Author's statement

Conflict of interest: Authors state no conflict of interest.

References

- [1] M. Utkur, Y. Muslu, and E. U. Saritas. Relaxation-based color magnetic particle imaging for viscosity mapping. *Applied Physics Letters*, 115(15):152403, 2019.
- [2] Z. W. Tay, P. W. Goodwill, D. W. Hensley, L. A. Taylor, B. Zheng, and S. M. Conolly. A high-throughput, arbitrary-waveform, mpi spectrometer and relaxometer for comprehensive magnetic particle optimization and characterization. *Scientific Reports*, 6(1):34180, 2016, doi:10.1038/srep34180.
- [3] C. B. Top. An arbitrary waveform magnetic nanoparticle relaxometer with an asymmetrical three-section gradiometric receive coil. *Turkish Journal of Electrical Engineering and Computer Science*, 28:1344–1354, 2020, doi:10.3906/elk-1907-201.
- [4] D. Pantke, N. Holle, A. Mogarkar, M. Straub, and V. Schulz. Multifrequency magnetic particle imaging enabled by a combined passive and active drive field feed-through compensation approach. *Medical physics*, 46(9):4077–4086, 2019.
- [5] Z. W. Tay, D. Hensley, J. Ma, P. Chandrasekharan, B. Zheng, P. Goodwill, and S. Conolly. Pulsed excitation in magnetic particle imaging. *IEEE transactions on medical imaging*, 38(10):2389–2399, 2019.
- [6] A. A. Ozasan, A. R. Cagil, M. Graeser, T. Knopp, and E. U. Saritas. Design of a magnetostimulation head coil with rutherford cable winding. *International Journal on Magnetic Particle Imaging*, 6(2 Suppl 1), 2020.

- [7] A. R. Çağıl and E. U. Saritas. Design of a preclinical field free point/field free line hybrid mpi scanner. *IWMPI*, 2019.
- [8] A. R. Çağıl, B. Tasdelen, and E. U. Saritas. Design of a doubly tunable gradiometer coil. *International Journal on Magnetic Particle Imaging*, 6(2 Suppl 1), 2020.
- [9] S. Kurt, Y. Muslu, and E. U. Saritas. Partial fov center imaging (pci): A robust x-space image reconstruction for magnetic particle imaging. *IEEE Transactions on Medical Imaging*, 39(11):3441–3450, 2020.